

# Weak effects in proton beam asymmetries at polarised RHIC and beyond

S. Moretti, M.R. Nolten and D.A. Ross

*School of Physics and Astronomy, University of Southampton  
Highfield, Southampton SO17 1BJ, UK*

## Abstract

We report on a calculation of the full one-loop weak corrections through the order  $\alpha_S^2\alpha_W$  to parton-parton scattering in all possible channels at the Relativistic Heavy Ion Collider (RHIC) running with polarised  $pp$  beams (RHIC-Spin). This study extends the analysis previously carried out for the case of  $2 \rightarrow 2$  subprocesses with two external gluons, by including all possible four-quark modes with and without an external gluon. The additional contributions due to the new four-quarks processes are extremely large, of order 50 to 100% (of either sign), not only in the case of parity-violating beam asymmetries but also for the parity-conserving ones and (although to a more limited extent) the total cross section. Such  $\mathcal{O}(\alpha_S^2\alpha_W)$  effects on the CP-violating observables would be an astounding 5 times larger for the case of the LHC with polarised beams – which has been discussed as one of the possible upgrades of the CERN machine – whereas they would be much reduced for the case of the CP-conserving ones as well as the cross section.

Keywords: Electroweak physics, Parity violation, Polarised  $pp$  scattering, RHIC

The purely weak component of Electro-Weak (EW) interactions is responsible for inducing parity-violating effects in jet observables, detectable through asymmetries in the cross section, which are often regarded as an indication of physics beyond the Standard Model (SM) [1]. These effects are further enhanced if polarisation of the incoming beams is exploited, like at the BNL machine mentioned in the abstract [2, 3]. There have also been some discussions [4, 5] on the idea of polarising the proton beams at the Large Hadron Collider (LHC) as one of the possible upgrades of the CERN machine, though no proposal has been put forward yet. At either machine, comparison of theoretical predictions involving parity-violation with experimental data can be used as a powerful tool for confirming or disproving the existence of some beyond the SM scenarios, such as those involving right-handed weak currents [6], contact interactions [7] and/or new massive gauge bosons [8, 9, 10].

In view of all this, it becomes of crucial importance to assess the quantitative relevance of weak effects entering via  $\mathcal{O}(\alpha_s^2\alpha_W)$  the fifteen possible  $2 \rightarrow 2$  partonic subprocesses responsible for jet production in hadronic collisions<sup>1</sup>, namely:

$$gg \rightarrow q\bar{q} \quad (1)$$

$$q\bar{q} \rightarrow gg \quad (2)$$

$$qg \rightarrow qg \quad (3)$$

$$\bar{q}g \rightarrow \bar{q}g \quad (4)$$

$$qq \rightarrow qq \quad (5)$$

$$\bar{q}\bar{q} \rightarrow \bar{q}\bar{q} \quad (6)$$

$$qQ \rightarrow qQ \text{ (same generation)} \quad (7)$$

$$\bar{q}\bar{Q} \rightarrow \bar{q}\bar{Q} \text{ (same generation)} \quad (8)$$

$$qQ \rightarrow qQ \text{ (different generation)} \quad (9)$$

$$\bar{q}\bar{Q} \rightarrow \bar{q}\bar{Q} \text{ (different generation)} \quad (10)$$

$$q\bar{q} \rightarrow q\bar{q} \quad (11)$$

$$q\bar{q} \rightarrow Q\bar{Q} \text{ (same generation)} \quad (12)$$

$$q\bar{q} \rightarrow Q\bar{Q} \text{ (different generation)} \quad (13)$$

$$q\bar{Q} \rightarrow q\bar{Q} \text{ (same generation)} \quad (14)$$

$$q\bar{Q} \rightarrow q\bar{Q} \text{ (different generation)}, \quad (15)$$

with  $q$  and  $Q$  referring to quarks of different flavours, limited to  $u$ -,  $d$ -,  $s$ -,  $c$ - and  $b$ -type (all taken as massless). While the first four processes (with external gluons) were already computed in Ref. [3], the eleven four-quark processes are new to this study<sup>2</sup>. Besides, these four-quark processes can be (soft and collinear) infrared divergent, so that gluon bremsstrahlung effects ought to be evaluated to obtain a finite cross section at the considered order. In addition, for completeness, we have also included the non-divergent  $2 \rightarrow 3$  subprocesses

$$qg \rightarrow qq\bar{q} \quad (16)$$

---

<sup>1</sup>Note that in our treatment we identify the jets with the partons from which they originate.

<sup>2</sup>Note that  $gg \rightarrow gg$  does not appear through  $\mathcal{O}(\alpha_s^2\alpha_W)$  nor do  $qq' \rightarrow QQ'$ ,  $\bar{q}\bar{q}' \rightarrow \bar{Q}\bar{Q}'$  and  $q\bar{q}' \rightarrow Q\bar{Q}'$ .

$$\bar{q}g \rightarrow \bar{q}\bar{q}q \quad (17)$$

$$qg \rightarrow qQ\bar{Q} \text{ (same generation)} \quad (18)$$

$$\bar{q}g \rightarrow \bar{q}\bar{Q}Q \text{ (same generation)}. \quad (19)$$

By recalling that at the typical RHIC-Spin energies (e.g.,  $\sqrt{s} = 300$  and  $600$  GeV) the quark luminosity is much larger than the gluon one, it is clear that are processes with oncoming quarks that dominate the phenomenology of jet production here. In contrast, at the LHC ( $\sqrt{s} = 14$  TeV), gluon-induced processes are largely dominant, particularly at low Bjorken- $x$ . As for what concerns the processes with external gluons, it is worth noticing that no CP-violation occurs at tree-level, so that  $\mathcal{O}(\alpha_S^2\alpha_W)$  is the first non-trivial order at which parity violation is manifest. Regarding four-quark processes, the following should be noted. Parity-violating contributions to channels (5)–(15) are induced already at tree-level, through  $\mathcal{O}(\alpha_{EW}^2)$ . Besides, all four-quark channels also exist through the CP-violating  $\mathcal{O}(\alpha_S\alpha_{EW})$  [11], although subprocesses (9), (10), (13) and (15) only receive Cabibbo-Kobayashi-Maskawa (CKM) suppressed contributions at this accuracy (i.e., they mainly proceed via CP-conserving  $\mathcal{O}(\alpha_S^2)$  interactions). Furthermore, notice in general that through  $\mathcal{O}(\alpha_S^2\alpha_W)$  there are many more diagrams available for channels (1)–(15) than via  $\mathcal{O}(\alpha_S^2)$  or indeed  $\mathcal{O}(\alpha_S\alpha_{EW})$  and  $\mathcal{O}(\alpha_{EW}^2)$ . Therefore, in terms of parton luminosity, simple combinatorics and power counting, one should expect the impact of  $\mathcal{O}(\alpha_S^2\alpha_W)$  terms to be large, certainly in parity-violating observables and possibly in parity-conserving ones as well. This is what we set out to test in this paper<sup>3</sup> for the case of RHIC and LHC. (See Refs. [12, 13] for an account of these effects at Tevatron.)

Before proceeding further we ought to clarify at this stage that we have only computed purely weak effects at one-loop level through  $\mathcal{O}(\alpha_S^2\alpha_W)$ , while in the case of tree-level processes via  $\mathcal{O}(\alpha_S\alpha_{EW})$  and  $\mathcal{O}(\alpha_{EW}^2)$  also the Electro-Magnetic (EM) contributions are included (and so are the interference effects between the two). This is why we are referring in this paper to the purely weak terms by adopting the symbol  $\alpha_W$ , while reserving the notation  $\alpha_{EW}$  for the full EW corrections. Here then, we will have  $\alpha_W \equiv \alpha_{EM}/\sin^2\theta_W$  (with  $\alpha_{EM}$  the Electro-Magnetic (EM) coupling constant and  $\theta_W$  the weak mixing angle) while  $\alpha_{EW}$  will refer to the appropriate composition of QED and weak effects as dictated by the SM dynamics.

We have not computed one-loop EM effects for two reasons. Firstly, their computation would be technically very challenging, because the photon in the loop can become infrared (i.e., soft and collinear) divergent, thus requiring also the inclusion of photon bremsstrahlung effects, other than of gluon radiation. Secondly,  $\mathcal{O}(\alpha_S^2\alpha_{EM})$  terms (in the above spirit,  $\alpha_{EM}$  signifies here only the contribution of purely EM interactions) would carry no parity-violating effects and their contribution to parity-conserving observables would anyway be overwhelmed by the well known  $\mathcal{O}(\alpha_S^3)$  terms [14] (see also [15, 16]). However, notice that we are not including these next-to-leading order (NLO) QCD corrections either, as we are mainly interested in parity-violating beam asymmetries.

Since we are considering weak corrections that may be identified via their induced parity-violating effects and since we wish to apply our results to the case of polarised proton beams, it is convenient to work in terms of helicity Matrix Elements (MEs). Here, we define the helicity

---

<sup>3</sup>Subprocesses (16)–(19) turn out to be numerically negligible at both machines and whichever the observable, so that we will not consider them in the remainder.

amplitudes by using the formalism discussed in Ref. [17]. At one-loop level such helicity amplitudes acquire higher order corrections from: (i) self-energy insertions on the fermions and gauge bosons; (ii) vertex corrections and (iii) box diagrams. The expressions for each of the corresponding one-loop amplitudes have been calculated using FORM [18] and checked by an independent program based on FeynCalc [19]. Internal gauge invariance tests have also been performed. The full expressions for the contributions from these graphs are however too lengthy to be reproduced here.

As already mentioned, infrared divergences occur when the virtual or real (bremsstrahlung) gluon is either soft or collinear with the emitting parton and these have been dealt with by using the formalism of Ref. [20], whereby corresponding dipole terms are subtracted from the bremsstrahlung contributions in order to render the phase space integral free of infrared divergences. The integrations over the gluon phase space of these dipole terms were performed analytically in  $d$ -dimensions, yielding pole terms which cancelled explicitly against those of the virtual graphs. There remains a divergence from the initial state collinear configuration, which is absorbed into the scale dependence of the Parton Distribution Functions (PDFs) and must be matched to the scale at which these PDFs are extracted. Recall that the remnant initial state collinear divergence at  $\mathcal{O}(\alpha_s)$  is absorbed by the LO  $Q^2$  dependence of the PDFs. Therefore, to  $\mathcal{O}(\alpha_s^2\alpha_W)$ , it is sufficient, for the purpose of matching these divergences, to consider the LO PDFs. It is also consistent to use the values of the running  $\alpha_s$  obtained from the one-loop  $\beta$ -function. In order to display the corrections due to genuine weak interactions the same PDFs and strong coupling are used in the LO and NLO observables.

The self-energy and vertex correction graphs contain ultraviolet divergences that have been subtracted here by using the ‘modified’ Dimensional Reduction ( $\overline{\text{DR}}$ ) scheme at the scale  $\mu = M_Z$ . The use of  $\overline{\text{DR}}$ , as opposed to the more usual ‘modified’ Minimal Subtraction ( $\overline{\text{MS}}$ ) scheme, is forced upon us by the fact that the  $W$ - and  $Z$ -bosons contain axial couplings which cannot be consistently treated in ordinary dimensional regularisation. Thus the values taken for the running  $\alpha_s$  refer to the  $\overline{\text{DR}}$  scheme whereas the EM coupling,  $\alpha_{\text{EM}}$ , has been taken to be  $1/128$  at the above subtraction point. The one exception to this renormalisation scheme has been the case of the self-energy insertions on external fermion lines, which have been subtracted on mass-shell, so that the external fermion fields create or destroy particle states with the correct normalisation

The top quark entering the loops in reactions with external  $b$ ’s has been assumed to have mass  $m_t = 175$  GeV and width  $\Gamma_t = 1.55$  GeV. The  $Z$  mass used was  $M_Z = 91.19$  GeV and was related to the  $W$ -mass,  $M_W$ , via the SM formula  $M_W = M_Z \cos \theta_W$ , where  $\sin 2\theta_W = 0.232$ . (Corresponding widths were  $\Gamma_Z = 2.5$  GeV and  $\Gamma_W = 2.08$  GeV.) For the strong coupling constant,  $\alpha_s$ , we have used the one-loop expression with  $\Lambda_{\overline{\text{MS}}}^{(n_f=4)}$  chosen to match the value required by the (LO) PDFs used. The latter were Gehrmann-Stirling set A (GSA) [21] and Glück-Reya-Stratmann-Vogelsang standard set (GRSV-STN) [22].

The following beam asymmetries, e.g., can be defined, depending on whether one or both beams are polarised:

$$\begin{aligned} A_{LL} d\sigma &\equiv d\sigma_{++} - d\sigma_{+-} \\ &\quad + d\sigma_{--} - d\sigma_{-+}, \\ A_L d\sigma &\equiv d\sigma_- - d\sigma_+, \end{aligned}$$

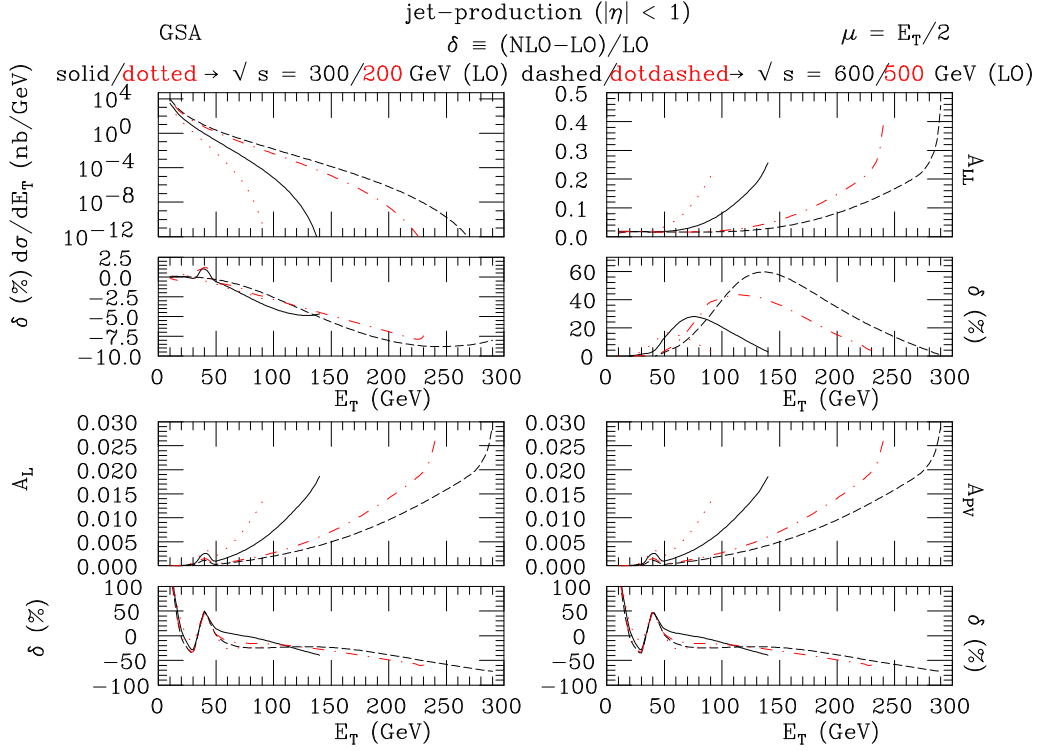


Figure 1: The dependence of the cross section as well as of the beam asymmetries on the jet transverse energy at tree-level (large frames) and the size of the one-loop weak corrections (small frames), at the two RHIC-Spin energies  $\sqrt{s} = 300$  and  $600$  GeV. Notice that the pseudo-rapidity range of the jets is limited to  $|\eta| < 1$  and the standard jet cone requirement  $\Delta R > 0.7$  is imposed as well (although we eventually sum the two- and three-jet contributions). We use GSA as PDFs and  $\mu = E_T/2$  as factorisation/renormalisation scale. Corresponding results for other two energy options (mentioned later on)  $\sqrt{s} = 200$  and  $500$  GeV are also given.

$$A_{PV} d\sigma \equiv d\sigma_{--} - d\sigma_{++}. \quad (20)$$

The first is parity-conserving while the last two are parity-violating<sup>4</sup>.

Figs. 1 shows the size of the  $\mathcal{O}(\alpha_S^2\alpha_W)$  effects relatively to the well known LO results, the latter being defined as the sum of all  $\mathcal{O}(\alpha_S^2)$ ,  $\mathcal{O}(\alpha_S\alpha_{EW})$  and  $\mathcal{O}(\alpha_{EW}^2)$  contributions, for the case of RHIC, for two reference energies. Both the differential cross section and the above beam asymmetries are plotted, each as a function of the jet transverse energy. The  $\mathcal{O}(\alpha_S^2\alpha_W)$  corrections are already very large at cross section level, by reaching  $-5(-9)\%$  at  $\sqrt{s} = 300(600)$  GeV, in the vicinity of  $E_T = 120(240)$  GeV. Effects onto the  $A_{LL}$  asymmetry are even larger, with maxima of  $\approx 25(60)\%$  for  $E_T \approx 70(140)$  GeV, again, in correspondence of  $\sqrt{s} = 300(600)$  GeV. In the case of both  $A_L$  and  $A_{PV}$ , in regions away from the threshold at  $E_T \approx M_W/4$  (where resonance effects emerge), there is no local maximum for positive or negative corrections, as both grow monotonically to the level of  $+100\%$  (at low  $E_T$ ) and  $-50$  to  $-70\%$  (at high  $E_T$  and with increasing collider energy). All such effects should comfortably be observable at RHIC, for the customary values of integrated luminosity, of  $200$  and  $800$   $\text{pb}^{-1}$ , in correspondence of  $\sqrt{s} = 300$  and  $600$  GeV [1].

<sup>4</sup>In the numerical analysis which follows we will assume 100% polarisation of the beams.

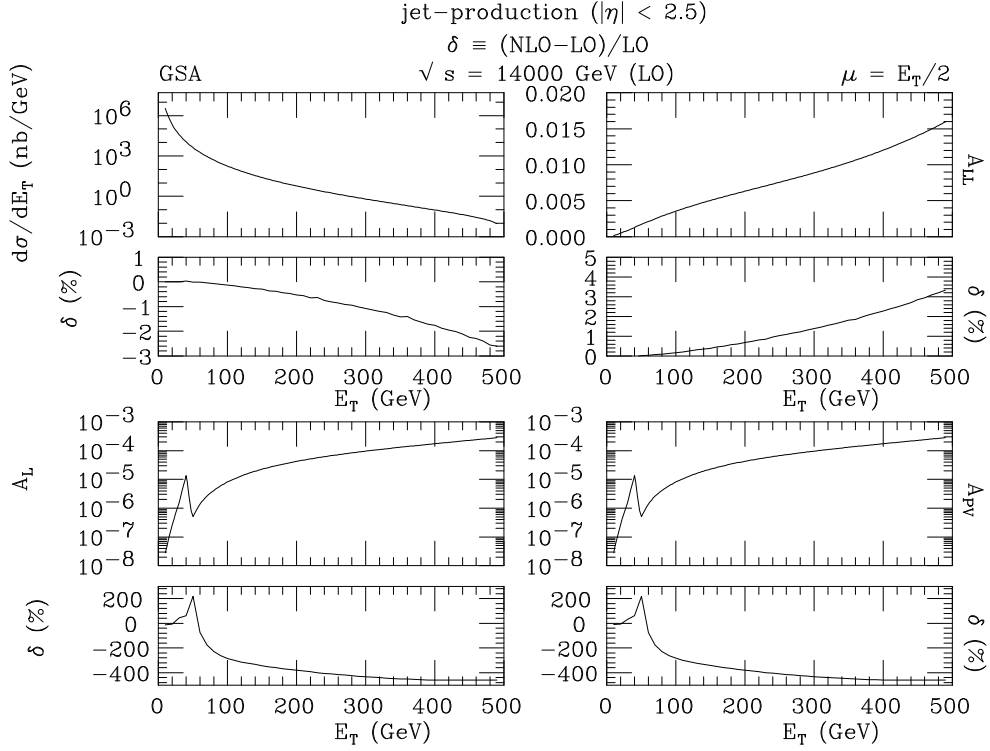


Figure 2: The dependence of the cross section as well as of the beam asymmetries on the jet transverse energy at tree-level (large frames) and the size of the one-loop weak corrections (small frames), at the LHC energy  $\sqrt{s} = 14$  TeV. Notice that the pseudo-rapidity range of the jets is limited to  $|\eta| < 2.5$  and the standard jet cone requirement  $\Delta R > 0.7$  is imposed as well (although we eventually sum the two- and three-jet contributions). We use GSA as PDFs and  $\mu = E_T/2$  as factorisation/renormalisation scale.

At the LHC with polarised beams (but standard energy  $\sqrt{s} = 14$  TeV), the  $\mathcal{O}(\alpha_s^2\alpha_W)$  corrections to the total cross section as well as the CP-conserving asymmetry are reasonably under control. In fact, they grow monotonically and reach the  $\approx -3\%$  and  $\approx 4\%$  at the kinematic limit of the jet transverse energy (as defined by the PDFs), respectively. However, it is debatable as to whether these effects can actually be disentangled, as we expect systematic experimental uncertainties to be of the same order. Away from the threshold at  $E_T \approx M_W/2$ ,  $\mathcal{O}(\alpha_s^2\alpha_W)$  effects onto the parity-violating asymmetries are instead enormous, as they yield a  $K$ -factor increasing from  $-2$  to  $-4.5$ , as  $E_T$  varies from 80 to 500 GeV. Despite the absolute value of the CP-violating asymmetries is rather small in the above interval, the huge LHC luminosity ( $10 \text{ fb}^{-1}$  per year should be feasible for, say, a 70% polarisation per beam [23]) would render the above higher order corrections manifest.

It is intriguing to understand the different behaviours of the  $\mathcal{O}(\alpha_s^2\alpha_W)$  effects depending on the observable and the collider being considered. To this end, we have presented in Tabs. 1–2 the contributions to the  $E_T$  dependent cross section of subprocesses (1)–(15) through  $\mathcal{O}(\alpha_s^2\alpha_W)$  separately, at both RHIC-Spin and LHC. The purpose of these tables is to illustrate that the leading partonic composition of the  $\mathcal{O}(\alpha_s^2\alpha_W)$  corrections is markedly different at the two machines. While at RHIC the key role is played by subprocess (7), at the LHC the conspicuous rise of the gluon-luminosity enhances in turn the yield of channel (3) to a level comparable

to that of mode (7)<sup>5</sup>. (The hierarchy among the subprocesses seen in Tabs. 1–2, for fixed jet transverse energy, is characteristic across most of the available  $E_T$  range at both colliders.) The  $\mathcal{O}(\alpha_s^2\alpha_W)$  corrections are particularly large for subprocesses (7)–(8) and (12), mainly in virtue of the large combinatorics involved at loop level (as intimated earlier), with respect to the LO case.

Table 1: The contributions of subprocesses (1)–(15) to order  $\alpha_s^2\alpha_W$  with respect to the full LO result for the total cross section at RHIC-Spin, at  $E_T = 70$  GeV for  $\sqrt{s} = 300$  GeV and  $E_T = 140$  GeV for  $\sqrt{s} = 600$  GeV. Here, we have paired together the channels with identical Feynman diagram topology. We use GSA as PDFs and  $\mu = E_T/2$  as factorisation/renormalisation scale. Column (a) is the percentage contribution from the  $\mathcal{O}(\alpha_s^2\alpha_W)$  corrections, column (b) is the percentage correction to the tree-level partonic subprocess and column (c) is the percentage contribution at the tree-level of that partonic subprocess to the differential cross section at the relevant  $E_T$ .

Subprocess	$\sqrt{s} = 300$ GeV			$\sqrt{s} = 600$ GeV		
	(a)	(b)	(c)	(a)	(b)	(c)
$gg \rightarrow gg$			1.35			1.17
(1)	1.73E-05	0.0267	0.0650	−0.000101	−0.179	0.0565
(2)	4.72E-05	0.0253	0.188	−0.000331	−0.179	0.184
(3)–(4)	−0.0144	−0.0589	24.7	−0.0608	−0.264	23.0
(5)–(6)	−0.411	−0.899	46.1	−1.42	−3.00	47.1
(7)–(8)	−1.57	−6.64	23.8	−3.65	−14.7	24.6
(9)–(10)	0.000393	0.0551	0.718	−0.00602	−0.843	0.711
(11)	−0.00236	−0.252	0.946	−0.00664	−0.714	0.927
(12)	0.00664	10.90	0.0613	0.0146	25.5	0.0571
(13)	0.00222	1.23	0.182	0.00199	1.17	0.169
(14)	0.0406	3.20	1.28	0.0282	2.24	1.25
(15)	0.000350	0.0491	0.717	−0.00572	−0.803	0.708
$qq' \rightarrow QQ'$ or $\bar{q}\bar{q}' \rightarrow QQ'$			0.00710			0.0148
$q\bar{q}' \rightarrow QQ'$			0.00234			0.00131
Total	−1.94			−5.11		

The different behaviours seen in Figs. 1–2 can easily be interpreted in terms of the LO contributions. In this respect, as already mentioned, Tabs. 1–2 clearly make the point that the jet phenomenology at RHIC-Spin is dominated by subprocesses initiated by quarks only while at the LHC gluons-induced channels are generally predominant. At RHIC energies, LO production through order  $\alpha_s^2$  is dominated by channel (5) whereas at the LHC the overwhelmingly dominant  $\alpha_s^2$  channels are  $gg \rightarrow gg$  (which is not subject to  $\mathcal{O}(\alpha_s^2\alpha_W)$  corrections, as already mentioned) and subprocess (3). Besides, channel (5) through  $\mathcal{O}(\alpha_s^2)$  is mainly concentrated

<sup>5</sup>The relevance of the latter throughout originates from the combination of a always sizable valence quark luminosity and a large Feynman diagram combinatorics, as opposed to, e.g., a gluon luminosity steeply increasing with the collider energy but combined with a small numbers of graphs [3].

Table 2: The contributions of subprocesses (1)–(15) to order  $\alpha_S^2\alpha_W$  with respect to the full LO result for the total cross section at LHC, at  $E_T = 300$  GeV for  $\sqrt{s} = 14$  TeV. Here, we have paired together the channels with identical Feynman diagram topology. We use GSA as PDFs and  $\mu = E_T/2$  as factorisation/renormalisation scale. Column (a) is the percentage contribution from the  $\mathcal{O}(\alpha_S^2\alpha_W)$  corrections, column (b) is the percentage correction to the tree-level partonic subprocess and column (c) is the percentage contribution at the tree-level of that partonic subprocess to the differential cross section at the relevant  $E_T$ .

Subprocess	$\sqrt{s} = 14$ TeV		
	(a)	(b)	(c)
$gg \rightarrow gg$			41.9
(1)	−0.0315	−1.25	1.89
(2)	−0.00386	−1.27	0.228
(3)–(4)	−0.455	−0.711	47.8
(5)–(6)	−0.112	−4.92	1.70
(7)–(8)	−0.431	−17.3	1.87
(9)–(10)	−0.0330	−2.67	0.926
(11)	−0.0328	−1.85	1.328
(12)	0.0466	64.8	0.0540
(13)	−0.00316	−1.50	0.158
(14)	0.0131	0.821	1.196
(15)	−0.0325	−2.64	0.924
$qq' \rightarrow QQ'$ or $\bar{q}\bar{q}' \rightarrow QQ'$			0.0221
$q\bar{q}' \rightarrow QQ'$			0.000979
Total	−1.075		

at low  $E_T$  while with growing  $E_T$  the  $\mathcal{O}(\alpha_S\alpha_{EW})$  and – particularly –  $\mathcal{O}(\alpha_{EW}^2)$  terms gain in relative importance. Furthermore,  $\mathcal{O}(\alpha_S^2)$  terms entering channel (5) do not contribute, obviously, to the parity-violating asymmetries. Therefore, it should not be surprising to see at RHIC-Spin that our corrections are very large in the case of the latter, where the LO term is  $\mathcal{O}(\alpha_S\alpha_{EW})$ , respect to which the corrections computed here are suppressed only by one power of  $\alpha_S$ . We attribute instead the size of the  $\mathcal{O}(\alpha_S^2\alpha_W)$  effects on the cross section and the parity-conserving asymmetry again to the fact that through  $\mathcal{O}(\alpha_S^2\alpha_W)$  there are many more diagrams available for such channels than via  $\mathcal{O}(\alpha_S^2)$  or indeed  $\mathcal{O}(\alpha_S\alpha_{EW})$  and  $\mathcal{O}(\alpha_{EW}^2)$ . As for the LHC, the fact that  $gg \rightarrow gg$  and subprocess (3) vastly dominates through  $\mathcal{O}(\alpha_S^2)$  the  $d\sigma/dE_T$  distribution explains why  $\mathcal{O}(\alpha_S^2\alpha_W)$  corrections are limited to the percent level. In  $A_{LL}$ , which has no  $gg \rightarrow gg$  component,  $\mathcal{O}(\alpha_S^2\alpha_W)$  effects become somewhat more visible in comparison.

Furthermore, in the case of the LHC, one should note the monotonic rise of the corrections with increasing jet transverse energy, for all observables studied, which can be attributed to the so-called Sudakov (leading) logarithms [24, 25] of the form  $\alpha_W \log^2(E_T^2/M_W^2)$ , which appear



in the presence of higher order weak corrections. These ‘double logarithms’ are due to a lack of cancellation of infrared (both soft and collinear) virtual and real emission in higher order contributions due to  $W$ -exchange, arising from a violation of the Bloch-Nordsieck theorem occurring in non-Abelian theories. (In fact, if events with real  $Z$  radiation are vetoed in the jet sample,  $\alpha_W \log^2(E_T/M_Z^2)$  terms would also affect the corrections [12].) Clearly, at LHC energies,  $E_T$  can be very large, thus probing the kinematic regime of these logarithmic effects, which instead affected RHIC only very mildly. Combine then the effects of such large logarithms with the fact that  $A_L$  and  $A_{PV}$  receive no pure QCD contributions, and one can explain the enormous (and increasing with  $E_T$ )  $\mathcal{O}(\alpha_S^2 \alpha_W)$  corrections to these two observables. In fact, recall that another way of viewing the  $\mathcal{O}(\alpha_S^2 \alpha_W)$  terms computed here is as first order QCD corrections to the  $\mathcal{O}(\alpha_S \alpha_W)$  terms, which are the leading order contributions to  $A_L$  and  $A_{PV}$ . From this perspective then, the large results reported here can be understood as large  $\mathcal{O}(\alpha_S)$  corrections. Furthermore, also recall here the following two aspects, already mentioned. Firstly, there are several partonic processes which are CKM suppressed at  $\mathcal{O}(\alpha_S \alpha_{EW})$  but which occur without CKM suppression at  $\mathcal{O}(\alpha_S^2 \alpha_W)$ . Secondly, processes involving external gluons and weak interactions occur for the first time at  $\mathcal{O}(\alpha_S^2 \alpha_W)$ .

As one of the purposes of polarised colliders is to measure polarised structure functions, in the ultimate attempt to reconstruct the proton spin, it is of some relevance to see how the  $\mathcal{O}(\alpha_S^2 \alpha_W)$  results obtained so far for GSA compare against GRSV-STN. This is done in Figs. 3–4, where we have also adopted the different choice  $\mu = E_{cm}(E_T)$  as factorisation/renormalisation scale, i.e., the centre-of-mass energy at parton level  $\sqrt{\hat{s}}$  (jet transverse energy), for the GSA(GRSV-STN) set. A comparison between the GSA curves in Figs. 3–4 and those in Figs. 1–2 reveals that the scale dependence of our corrections is not very substantial for a given PDF set (the same is true for the case of GRSV-STN). In contrast, depending on the choice of PDFs, corrections through  $\mathcal{O}(\alpha_S^2 \alpha_W)$  can be very different for each observables studied at both RHIC-Spin and LHC, with the exception of the cross section in either case.

Altogether, the results presented here point to the extreme relevance of one-loop  $\mathcal{O}(\alpha_S \alpha_W^2)$  weak contributions for precision analyses of jet data produced in polarised proton-proton scattering at RHIC. We have confirmed that this would be the case also at a polarised LHC, which has been discussed as one of the possible upgrades of the CERN collider. The size of the afore-mentioned corrections, relative to the lowest order results, is rather insensitive to the choice of factorisation/renormalisation scale, yet it shows some sizable dependence on the polarised PDFs used. EM effects were neglected here because they are not subject to parity-violating effects. However, their computation is currently in progress. The inclusion of NLO terms from pure QCD, through  $\mathcal{O}(\alpha_S^3)$ , is also in order, as they can produce effects of order 100%, even to the parity-violating asymmetries, though in this case they will only amount to a rescaling (within a factor of 2 at the most) of the normalisation, not to a change in shape. We are now working towards the full  $\mathcal{O}(\alpha_S^3)$  results including beam polarisation effects [26].

Finally, extrapolation of our results to other collider energies, chiefly for RHIC, for operation at  $\sqrt{s} = 200$  and 500 GeV, is straightforward. As expected, these results do not differ dramatically from those obtained for 300 and 600 GeV, respectively. Fig. 1 also shows the size of the corrections at these two additional energies, for our usual observables and default choice of PDFs and factorisation/renormalisation scale. For the purpose of emulating the effects of  $\mathcal{O}(\alpha_S \alpha_W^2)$  terms at whichever collider and energy, we make available our code on request.

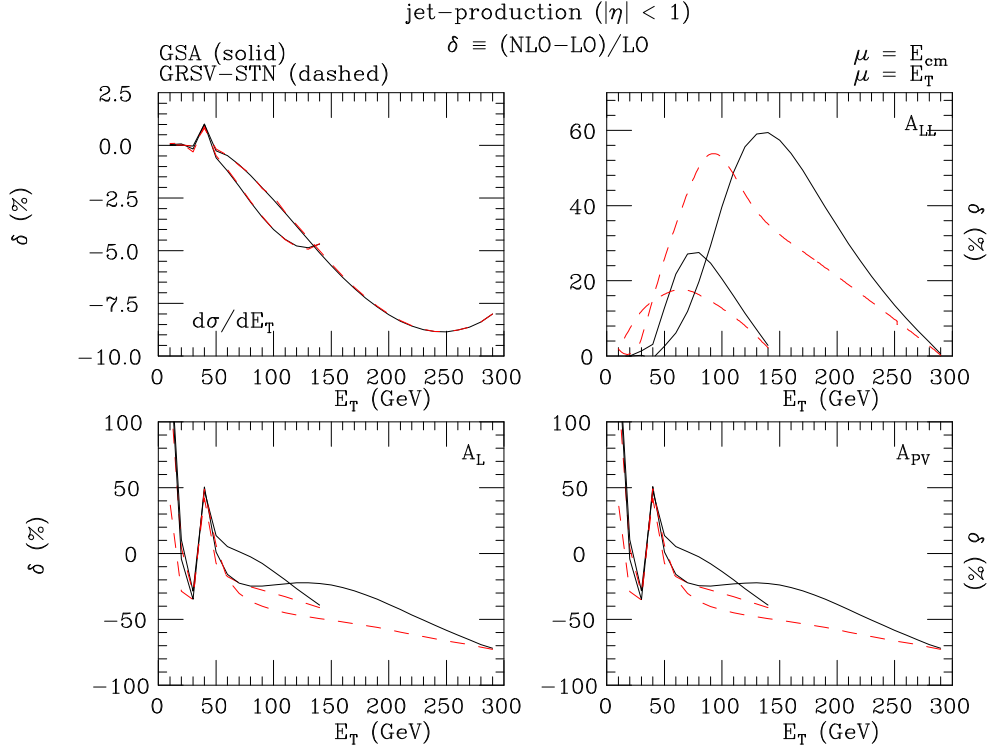


Figure 3: The dependence of the corrections to the cross section as well as the beam asymmetries on the jet transverse energy for two sets of PDFs, GSA and GRSV-STN, at the two RHIC-Spin energies  $\sqrt{s} = 300$  (curves extending to 150 GeV) and 600 GeV (curves extending to 300 GeV). Notice that the pseudo-rapidity range of the jets is limited to  $|\eta| < 1$  and the standard jet cone requirement  $\Delta R > 0.7$  is imposed as well (although we eventually sum the two- and three-jet contributions). We use  $\mu = E_{\text{cm}}(E_T)$  as factorisation/renormalisation scale in the case of GSA(GRSV-STN).

## Acknowledgements

We thank Ezio Maina for collaborative work in the early stages of this analysis.

## References

- [1] G. Bunce, N. Saito, J. Soffer and W. Vogelsang, *Ann. Rev. Nucl. Part. Sci.* **50** (2000) 525; G. Altarelli and M.L. Mangano (eds.), *Proceedings of the Workshop on “Standard Model Physics (and More) at the LHC”*, Geneva 2000, CERN 2000-004, 9 May 2000.
- [2] C. Bourrely, J.P. Guillet and J. Soffer, *Nucl. Phys.* **B361** (1991) 72.
- [3] J.R. Ellis, S. Moretti and D.A. Ross, *JHEP* **0106** (2001) 043.
- [4] J. M. Virey and P. Taxil, *Nucl. Phys. Proc. Suppl.* **105** (2002) 150.
- [5] S. D. Bass and A. De Roeck, *Nucl. Phys. Proc. Suppl.* **105** (2002) 1.
- [6] P. Taxil and J.M. Virey, *Phys. Lett.* **B404** (1997) 302.

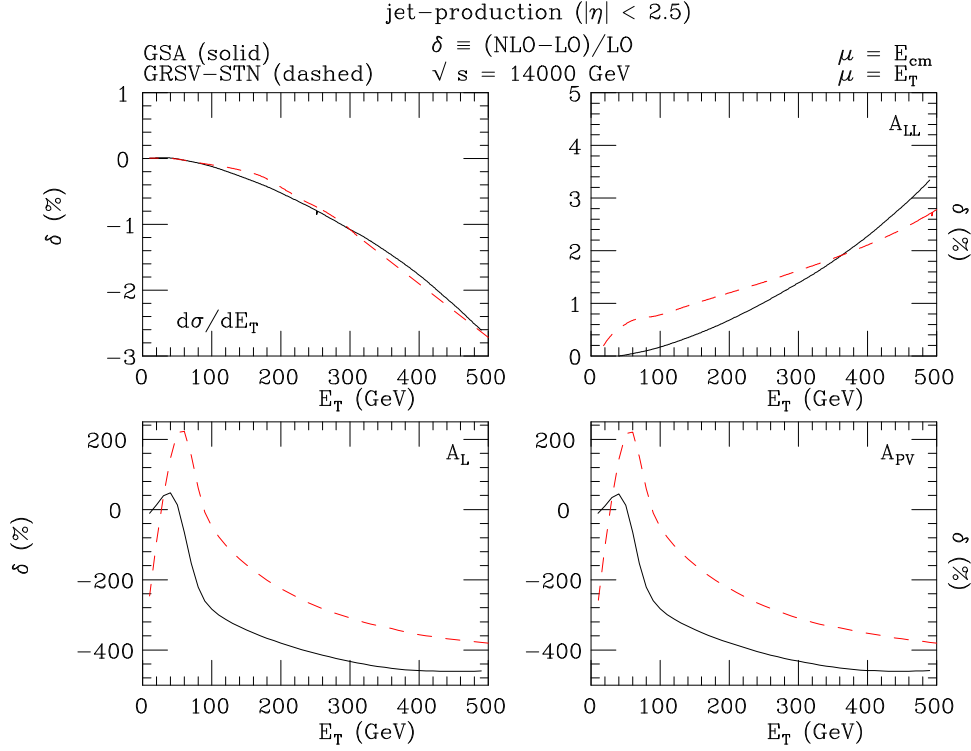


Figure 4: The dependence of the corrections to the cross section as well as the beam asymmetries on the jet transverse energy for two sets of PDFs, GSA and GRSV-STN, at the LHC energy  $\sqrt{s} = 14$  TeV. Notice that the pseudo-rapidity range of the jets is limited to  $|\eta| < 2.5$  and the standard jet cone requirement  $\Delta R > 0.7$  is imposed as well (although we eventually sum the two- and three-jet contributions). We use  $\mu = E_{\text{cm}}(E_T)$  as factorisation/renormalisation scale in the case of GSA(GRSV-STN).

- [7] P. Taxil and J.M. Virey, Phys. Rev. **D55** (1997) 4480.
- [8] P. Taxil and J.M. Virey, Phys. Lett. **B441** (1998) 376.
- [9] P. Taxil and J.M. Virey, Phys. Lett. **B383** (1996) 355.
- [10] M. Dittmar, A.S. Nicollerat and A. Djouadi, Phys. Lett. **B583** (2004) 111.
- [11] C. Bourrely, J.P. Guillet and J. Soffer, Nucl. Phys. **B361** (1991) 72.
- [12] S. Moretti, M.R. Nolten and D.A. Ross, hep-ph/0503152.
- [13] E. Maina, S. Moretti, M.R. Nolten and D.A. Ross, Phys. Lett. **B570** (2003) 205, hep-ph/0401093, hep-ph/0407150.
- [14] R. K. Ellis and J. C. Sexton, Nucl. Phys. **B269** (1986) 445.
- [15] S. D. Ellis, Z. Kunszt and D. E. Soper, Phys. Rev. Lett. **64** (1990) 2121.
- [16] W. T. Giele, E. W. N. Glover and D. A. Kosower, Phys. Rev. Lett. **73** (1994) 2019.

- [17] E. Maina, S. Moretti and D. A. Ross, JHEP **0304** (2003) 056.
- [18] J.A.M. Vermaseren, [math-ph/0010025](#).
- [19] J. Küblbeck, M. Böhm and A. Denner, Comput. Phys. Commun. **64** (1991) 165.
- [20] S. Catani and M. H. Seymour, Nucl. Phys. **B485** (1997) 291 [Erratum-ibid. **B510** (1997) 503].
- [21] T. Gehrmann and W.J. Stirling, Phys. Rev. **D53** (1996) 6100.
- [22] M. Glück, E. Reya, M. Stratmann and W. Vogelsang, Phys. Rev. **D63** (2001) 094005.
- [23] A. De Roeck, private communication.
- [24] M. Melles, Phys. Rept. **375** (2003) 219.
- [25] A. Denner, [hep-ph/0110155](#).
- [26] S. Moretti and D.A. Ross, in progress.